

## Tunable microwave magnetic properties in oblique deposited CoHf/Ta multilayers

Guozhi Chai, Xinhua Wang, Zhiling Wang, and Desheng Xue

Citation: *Journal of Applied Physics* **117**, 063901 (2015); doi: 10.1063/1.4907998

View online: <http://dx.doi.org/10.1063/1.4907998>

View Table of Contents: <http://scitation.aip.org/content/aip/journal/jap/117/6?ver=pdfcov>

Published by the [AIP Publishing](#)

---

### Articles you may be interested in

[Perpendicular magnetic anisotropy in Ta/Co<sub>2</sub>FeAl/MgO multilayers](#)

*J. Appl. Phys.* **114**, 063905 (2013); 10.1063/1.4818326

[Temperature-dependent dynamic magnetization of FeCoHf thin films fabricated by oblique deposition](#)

*J. Appl. Phys.* **112**, 083925 (2012); 10.1063/1.4763361

[Study on the soft magnetic properties and high frequency characteristics of Co-M \(M=Ti, Zr, and Hf\) thin films](#)

*J. Appl. Phys.* **111**, 07A333 (2012); 10.1063/1.3679157

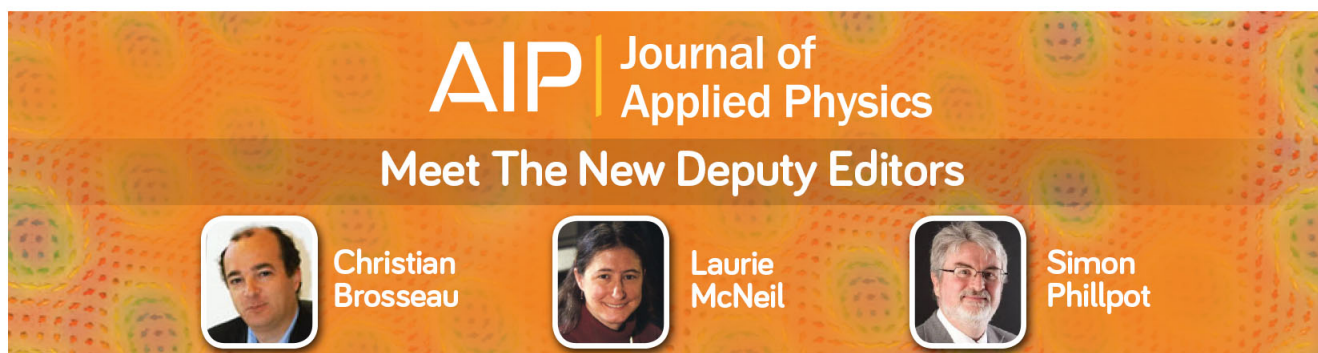
[Effect of thickness of MgO, Co-Fe-B, and Ta layers on perpendicular magnetic anisotropy of \[Ta/Co<sub>60</sub>Fe<sub>20</sub>B<sub>20</sub>/MgO\]<sub>5</sub> multilayered films](#)

*J. Appl. Phys.* **111**, 07C111 (2012); 10.1063/1.3673408

[Soft magnetism and microwave magnetic properties of Fe-Co-Hf films deposited by composition gradient sputtering](#)

*J. Appl. Phys.* **109**, 07A315 (2011); 10.1063/1.3549584

---

A promotional banner for the Journal of Applied Physics. It features the journal's logo at the top, followed by the text 'Meet The New Deputy Editors'. Below this, three circular headshots of the new deputy editors are shown, each with their name underneath: Christian Brosseau, Laurie McNeil, and Simon Phillpot. The background is a vibrant orange with a pattern of colorful, abstract shapes.

# Tunable microwave magnetic properties in oblique deposited CoHf/Ta multilayers

Guozhi Chai,<sup>a)</sup> Xinhua Wang, Zhiling Wang, and Desheng Xue<sup>a)</sup>

Key Laboratory for Magnetism and Magnetic Materials of the Ministry of Education, Lanzhou University, Lanzhou 730000, People's Republic of China

(Received 11 November 2014; accepted 31 January 2015; published online 10 February 2015)

In this work, the microwave magnetic properties of oblique deposited CoHf/Ta multilayers were investigated. The high frequency magnetic properties of CoHf/Ta multilayers showed different behaviors with oblique angle for different Ta interlayer thickness  $t$ . For example, when the Ta interlayer thickness fixed as 5.0 nm, the resonance frequency  $f_r$  increased from 2.1 to 3.4 GHz with the oblique deposition angle  $\theta$  changing from  $10^\circ$  to  $30^\circ$ . However, when the Ta layer fixed as 15.0 nm, the  $f_r$  decreased from 2.5 to 1.7 GHz with the oblique deposition angle changing in the same range. The opposite behavior of the  $f_r$  with  $\theta$  is supposed to result from the existence of the Ta buffer layer, in which the thicker Ta interlayer may hinder the self-shadow effects of the CoHf magnetic layers. © 2015 AIP Publishing LLC. [<http://dx.doi.org/10.1063/1.4907998>]

## I. INTRODUCTION

Magnetic thin films with tunable microwave magnetic properties are of great use for tunable microwave signal processing devices,<sup>1</sup> including tunable inductors,<sup>2,3</sup> tunable resonators,<sup>4</sup> phase shifters,<sup>5</sup> and tunable filters.<sup>6,7</sup> It is therefore necessary to have magnetic thin films whose ferromagnetic resonance (FMR) frequency and permeability can be tuned in an easy way. It is well known from Kittel's equation<sup>8</sup> that the FMR frequency and permeability are strongly dependent on the magnetic anisotropy and the saturation magnetization  $4\pi M_s$  of the films. While  $4\pi M_s$  is fixed by the material, the FMR frequency and permeability of the magnetic thin films can be tuned by changing the magnetic anisotropy via various methods such as *in situ* depositing on pre-stressed substrates,<sup>9</sup> exchange bias,<sup>10,11</sup> multilayer structure,<sup>12–15</sup> oblique deposition,<sup>16–19</sup> and gradient deposition.<sup>20–22</sup> Very recently, rotatable anisotropy has also been developed to tune the high frequency properties of ferrite doped CoFe thin films or thin films with rotatable stripe domain.<sup>23–26</sup> Each of the above methods has its own drawbacks: the pre-stressed substrates method requires the substrates to be flexible, exchange bias may only tune the anisotropy in ultra-thin films and the magnitude of rotatable anisotropy are relatively hard to control.<sup>9</sup> The origins of the rotatable anisotropy in different systems are still unclear and is hard to tune the value of the anisotropy in large ranges.<sup>23–26</sup> Thus, multilayers and oblique depositions are two most effective ways to tune the magnitude of anisotropy in regular thin films. In multilayers, the interlayer interactions of the magnetic layers can be changed by changing the thickness of the interlayer which led to the change of the anisotropy of the thin films. Then, the anisotropy of the films can be tuned by changing interlayer interactions. This effect has been found in many systems including CoNb/Ta multilayers,<sup>12</sup> CoFeZr/Cu multilayers,<sup>13</sup> CoZr/SiO<sub>2</sub> multilayers,<sup>14</sup>

and FeNiO/SiO<sub>2</sub> multilayers.<sup>15</sup> Oblique deposition is used to tune the anisotropy via the so-called self-shadow effect.<sup>16</sup> And the value of the anisotropy can be adjusted by controlling the oblique deposition angle. For example, the resonance frequency can be tuned from 2.4 to 3.8 GHz in CoFeHf thin films,<sup>17</sup> 1.3 to 4.9 GHz in CoNb thin films,<sup>18</sup> and 1.7 to 4.3 GHz in CoZr thin films.<sup>19</sup> Hence, it may be interesting to investigate the possibility of tuning the resonance frequency by combining these two ways. With these objectives in mind, we carry out in the present research work, a detailed investigation to see how the oblique deposition angle and the thickness of the interlayers affect both the static magnetic properties and high frequency characteristics of the oblique deposited CoHf/Ta multilayers and to discuss the results in light of the analysis based on the Landau-Lifshitz-Gilbert (LLG) equation.<sup>27</sup>

## II. EXPERIMENT

The radio frequency (RF) magnetron sputtering chamber was used to deposit (CoHf/Ta)<sub>8</sub> thin films at ambient temperature onto 5 mm × 5 mm × 0.42 mm Si(111) substrates with background pressure lower than  $5 \times 10^{-5}$  Pa. A 3-in. Ta target was used to deposit the Ta layers, and a 3-in. Co target with varying numbers of equal-sized 3 mm × 3 mm × 1 mm Hf chips attached was used to deposit CoHf layers. The compositions of the magnetic thin films were changed by controlling the number of Hf chips. During sputtering, an Ar flow rate of 20 SCCM (SCCM denotes cubic centimetre per minute at STP) was needed to maintain an Ar pressure of 0.2 Pa, and the RF power density was 1.7 W/cm<sup>2</sup>. The thickness of the thin films was controlled by the deposition time at a constant deposition rate, which was verified by a thickness profile meter. The structures of (CoHf/Ta)<sub>8</sub> multilayer thin films with Ta buffer layer can be found in Fig. 1. The first layer was 20 nm Ta buffer layer and subsequent (CoHf/Ta)<sub>8</sub> layers were deposited onto the previous Ta layer so that all the CoHf layers have the same interface conditions as the

<sup>a)</sup>Authors to whom correspondence should be addressed. Electronic addresses: chaigzh@lzu.edu.cn and xueds@lzu.edu.cn

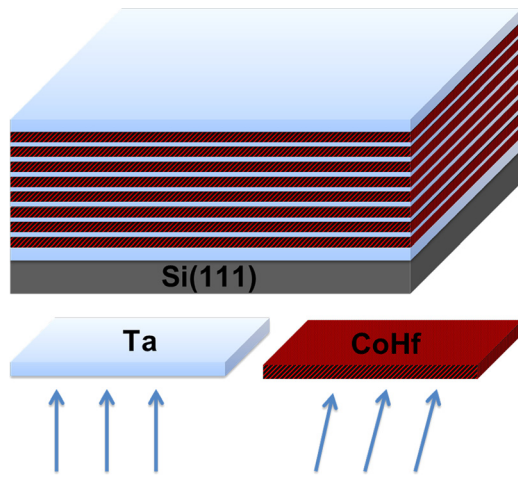


FIG. 1. The structures of  $(\text{CoHf/Ta})_8$  multilayer thin films with Ta buffer layer. The substrate is Si(111), CoHf layers were prepared with oblique deposition and Ta layers were prepared with normal deposition.

Ta-CoHf-Ta interfaces. A capping layer of Ta with thickness of 20 nm was deposited on top of the sample to protect them from oxidation. The thickness of each CoHf layer was fixed at 10 nm with the oblique deposition angle changing from  $0^\circ$  to  $30^\circ$ . The easy axis of the films induced by oblique deposition is perpendicular to the incident plane. The Ta interlayers were prepared by normal deposition changing the thickness from 10 to 1.0 nm for different samples.

The composition of the films was determined by energy dispersive X-ray spectroscopy (EDS). In this work, the composition of the CoHf layer is  $\text{Co}_{94}\text{Hf}_6$ . The  $M_s$  and M-H loops were obtained by the vibrating sample magnetometer (VSM Lakeshore model 7304). The  $H_k$  was determined by calculating the measured easy axis and hard axis loops of the reduced magnetization.<sup>28</sup> Permeability spectra were obtained by a vector network analyser using the room temperature

shorted microstrip transmission line<sup>29</sup> method with the frequency range from 100 MHz to 8 GHz.<sup>30</sup> The  $f_r$  and damping parameter  $\alpha$  were determined by fitting the permeability spectrum with theoretical equation derived from Landau-Lifshitz-Gilbert equation.<sup>27</sup>

### III. RESULTS AND DISCUSSIONS

First, the properties of single 80 nm CoHf thin film, which has the same thickness as the total thickness of the CoHf layers, were studied for comparison. The results of static magnetic properties can be found in Fig. 2. In Fig. 2(a), the easy axis M-H loop (EA) reveals typical easy axis loop of soft magnetic thin film with high remanence magnetization and low coercivity. The hard axis M-H loop (HA) is basically a closed curve with very small coercivity. The difference between the hysteresis loop along easy axis and hard axis indicates an in-plane uniaxial magnetic anisotropy in these CoHf thin films. In Fig. 2(b), the hysteresis loops of the hard axis with different oblique angles of CoHf were presented and the angles marked in the figure denote the oblique angle during deposition. The hard axis loops become more slanted with increasing oblique angles implying that the magnetic anisotropy increases with the increasing oblique angle. Thus, a monotonous increase of  $H_k$  as a function of oblique angle can be observed. For instance,  $H_k$  for CoHf film deposited at  $30^\circ$  is around 140 Oe, which is much larger than 33 Oe found in the film deposited at  $10^\circ$ . The real and imaginary parts of the permeability of CoHf thin film deposited under different oblique deposition angles are shown in Figs. 2(c) and 2(d). The resonance peak moves to a higher frequency range when the oblique angle becomes larger, which means the resonance frequency increases with the increasing oblique angle. This result is consistent with the Kittel equation. The real parts of the permeability decreases, while the resonance frequency

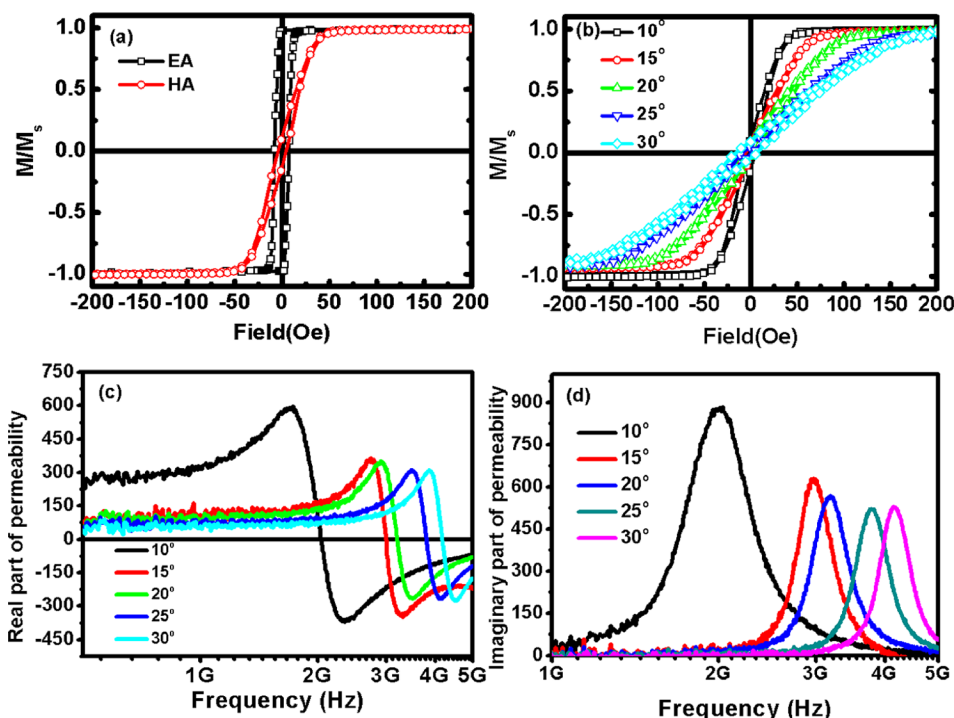


FIG. 2. The static and microwave magnetic properties of the single layer CoHf thin film with different oblique deposition angle. (a) Representative hysteresis loops of CoHf thin film. EA (HA) means the loops were measured by applying the field in easy axis (hard axis). (b) The hard axis loops of CoHf thin film deposited in different oblique deposition angles. The real (c) and imaginary (d) parts of permeability of CoHf thin film deposited under different oblique deposition angles.

increases, which is consistent with the Snoek's law that there exists a trade-off between permeability and resonance frequency.<sup>31</sup>

Next, we study the magnetic properties of multilayers with different interlayer thicknesses  $t$  deposited at different oblique angles. Figure 3 shows the high frequency permeability spectra of the CoHf/Ta multilayers with different oblique deposition angles. For multilayer with Ta interlayer thickness  $t$  of 5.0 nm, the behavior is similar with the single layer thin films, the peak of the imaginary part is shifted to higher frequency range when the oblique angle increases. It is indicated that resonance frequency increases with the increasing oblique deposition angle. The real parts of the permeability decrease, while the resonance frequency increases. However, it is interesting that when  $t$  increases to 15 nm, the peak of the imaginary part no longer increases with the increasing oblique angle, it shows a slightly decreasing behavior with the increasing oblique deposition angle, which means that the resonance frequency reduces with the increasing oblique deposition angle.

For more elaborate discussion on the behavior of both static and dynamic magnetic properties, we plot in Figure 4 a summary of the in-plane uniaxial anisotropy field  $H_k$ , coercivity  $H_c$ , and the resonance frequency  $f_r$  dependence on the oblique angle. The denotation of 0 nm Ta layer in this figure means the single layer CoHf film which has the same thickness as the total thickness of the CoHf layers in multilayer thin films. The anisotropy field shows a clear increase with oblique incidence angle for  $t < 5.0$  nm. However, the value of the anisotropy field does not change much while the interlayer thickness at a range  $7.5 \text{ nm} < t < 12.5$  nm. It is known that the in-plane uniaxial anisotropy in the oblique deposited thin films stems from the so-called self-shadow effect, which results in tilted columnar structure of the grains and sometimes with elongated columns.<sup>16,32,33</sup> With increasing Ta interlayer thickness, the thicker interlayers destroy the

regular array of the elongated columns and even destroy the growth of the columns. Furthermore, the thicker interlayer may decrease the interlayer interaction of the CoHf magnetic layers. Thus, the in-plane uniaxial anisotropy no longer increases with the oblique deposited angle due to the reasons discussed above. When  $t$  is increased to 15 nm, the resonance frequency shows a slightly decreasing behavior with the increasing oblique deposition angle. This means that the oblique deposited elongated columns are no longer the main cause of the anisotropy, so the anisotropy decreases for other unclear reasons, which need to be studied in our further research. The coercivity of single layer CoHf film and multilayer CoHf/Ta films dependence on the oblique angle are shown in Fig. 4(b). The values of coercivity of other multilayer films are similar with Ta thickness of 5 nm (only coercivity data for Ta thickness of 5 nm are shown in this figure). The coercivity of the films only changes in a small range of 2–12 Oe with the oblique angle increasing. This means that all these films are kept soft even though the anisotropy fields are increasing with the oblique angle. The behavior of the resonance frequency shows a similar behavior with anisotropy, which is consistent with the Kittel's equation.

It is known that the interlayer coupling will affect the effective uniaxial anisotropy of the multilayer thin films,<sup>12–15</sup> we thus plot the results of resonance frequency and the in-plane uniaxial anisotropy dependence on the interlayer thickness with fixed oblique deposition angles. The results can be found in Figure 5. The uniaxial anisotropy field  $H_k$  and the resonance frequency  $f_r$  decrease with the increasing Ta interlayer thickness from 0 to 15 nm when the oblique angle is larger than  $15^\circ$ , where 0 nm means the single layer thin film. These behaviors are the same as the other multilayer thin films.<sup>12–15</sup> It is known that the effective anisotropy has a relationship with the total energy density in the films. In multilayer thin films, the interlayer interaction energy becomes

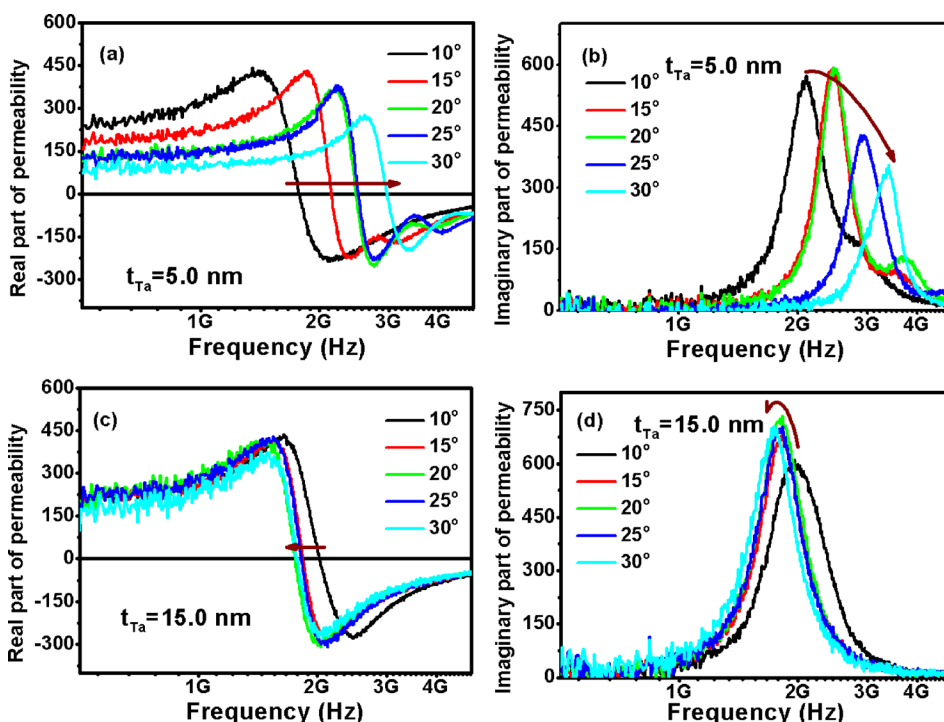


FIG. 3. High frequency permeability spectra of the multilayer CoHf/Ta thin film with different oblique deposition angle. (a) and (b) The real and imaginary parts of high frequency permeability spectra of CoHf/Ta thin film with Ta interlayer thickness as 5.0 nm. The angles shown in the figure means the oblique deposition angles. (c) and (d) The real and imaginary parts of high frequency permeability spectra of CoHf/Ta thin film with Ta interlayer thickness as 15.0 nm.

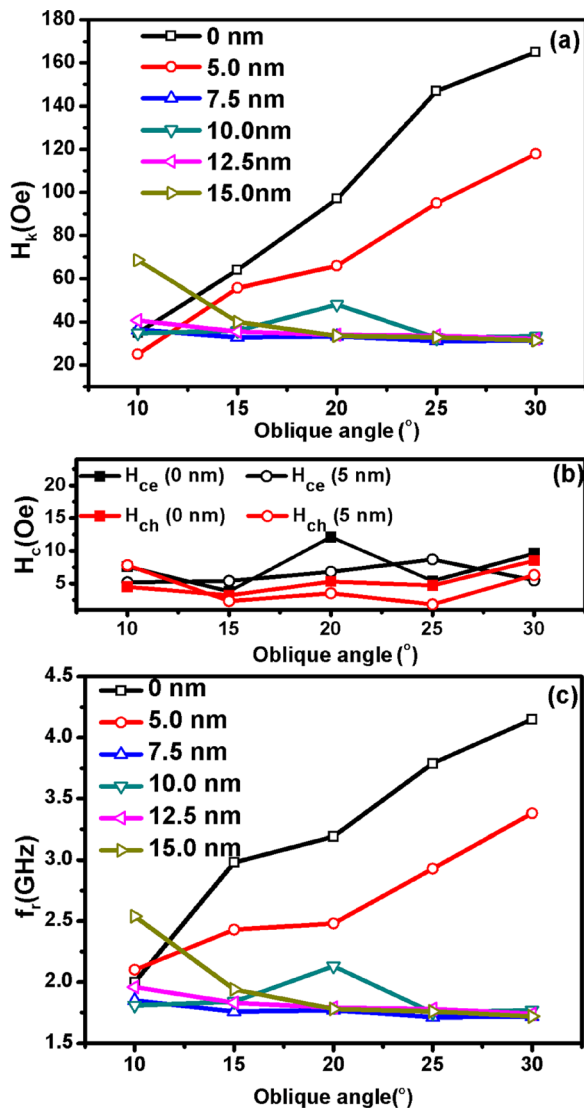


FIG. 4. Dependence of (a) the in-plane uniaxial anisotropy field  $H_k$  (b) the coercivity  $H_c$  and (c) the resonance frequency  $f_r$  on the oblique deposition angle in CoHf/Ta multilayer with different interlayer thickness.  $x$  nm in the figure means the interlayer thickness, 0 nm means the single layer CoHf film.

larger when the interlayer is thinner. Thus, the effective anisotropy field shows a decreasing behavior with the increasing interlayer thickness. However, for samples deposited with an oblique angle of 10°, the behavior shows a little difference. The  $H_k$  and  $f_r$  first decrease with the thickness of Ta layer increasing from 0 to 10 nm, then show a slight increasing behavior when the thickness of Ta layer increases from 10 to 15 nm. For this sample, the oblique deposition angle is so small that the self-shadow effect may no longer be the major effect for the effective anisotropy in the multilayers. Therefore, the behavior may be different compared with other samples with larger oblique deposition angles.

#### IV. SUMMARY

In summary, we have performed a detailed investigation of the influences of the oblique deposition angle and the interlayer thickness on the magnetic and microwave properties of CoHf/Ta multilayers. It is found that the oblique

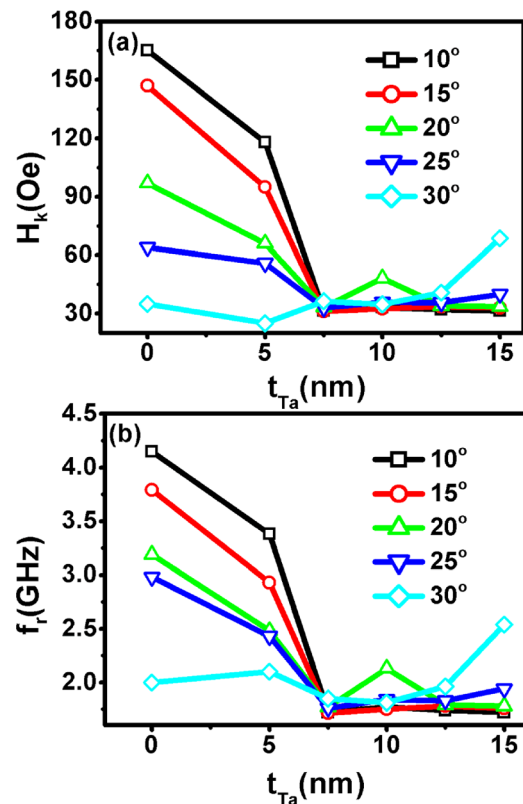


FIG. 5. Dependence of (a) the in-plane uniaxial anisotropy field  $H_k$  and (b) the resonance frequency  $f_r$  on the interlayer thickness CoHf/Ta multilayer with different oblique deposition angle. The value marked in the figure means the oblique deposition angle.

deposition angle can tailor the anisotropy significantly when the interlayer thickness is small, which is suggested to result from the formation of tilted columnar structure arising from self-shadow effect in oblique deposited films. For thicker interlayers, the anisotropy does not change very much with the oblique deposition angle as the thick interlayers may inhibit the growth of the columns and even destroy the regular array of the elongated columns. For multilayers with the same oblique deposition angle, the effective anisotropy decreases when the interlayer thickness is increased due to the reducing interlayer interaction. As a result, the resonance frequency can be tuned from 2.1 to 3.4 GHz, which is promising for microwave applications.

#### ACKNOWLEDGMENTS

The authors thank Mr. Wee Tee Soh for polishing the English. This work was supported by the National Basic Research Program of China (No. 2012CB933101), National Natural Science Foundation of China (NSFC) (Nos. 51107055, 51471080, 11034004, and 51371093), and the Fundamental Research Funds for the Central Universities (No. lzujbky-2014-40).

<sup>1</sup>N. X. Sun and G. Srinivasan, *SPIN* **2**, 1240004 (2012).

<sup>2</sup>J. Lou, D. Reed, M. Liu, and N. X. Sun, *Appl. Phys. Lett.* **94**, 112508 (2009).

<sup>3</sup>X. L. Li, G. Z. Chai, D. W. Guo, B. Gao, Z. M. Zhang, and D. S. Xue, *Microelectron. Eng.* **86**, 2290 (2009).

<sup>4</sup>Y. K. Fetisov and G. Srinivasan, *Appl. Phys. Lett.* **88**, 143503 (2006).

- <sup>5</sup>A. S. Tatarenko, G. Srinivasan, and M. I. Bichurin, *Appl. Phys. Lett.* **88**, 183507 (2006).
- <sup>6</sup>A. S. Tatarenko, V. Gheevarghese, and G. Srinivasan, *Electron. Lett.* **42**, 540 (2006).
- <sup>7</sup>C. Pettiford, S. Dasgupta, J. Lou, S. D. Yoon, and N. X. Sun, *IEEE Trans. Magn.* **43**, 3343 (2007).
- <sup>8</sup>C. Kittel, *Phys. Rev.* **71**, 270 (1947).
- <sup>9</sup>Y. Fu, Z. Yang, T. Miyao, M. Matsumoto, X. X. Liu, and A. Morisako, *Mater. Sci. Eng., B* **133**, 61 (2006).
- <sup>10</sup>J. McCord, R. Kaltofen, O. G. Schmidt, and L. Schultz, *Appl. Phys. Lett.* **92**, 162506 (2008).
- <sup>11</sup>N. N. Phuoc, F. Xu, and C. K. Ong, *Appl. Phys. Lett.* **94**, 092505 (2009).
- <sup>12</sup>G. Z. Chai, Y. C. Yang, J. Y. Zhu, M. Lin, W. B. Sui, D. W. Guo, X. L. Li, and D. S. Xue, *Appl. Phys. Lett.* **96**, 012505 (2010).
- <sup>13</sup>G. Z. Chai, Z. L. Wang, G. X. Wang, W. B. Sui, and D. S. Xue, *IEEE Trans. Magn.* **47**, 3115 (2011).
- <sup>14</sup>X. H. Wang, G. Z. Chai, and D. S. Xue, *J. Alloys Compd.* **584**, 171 (2014).
- <sup>15</sup>H. Geng, J. Q. Wei, S. J. Nie, Y. Wang, Z. W. Wang, L. S. Wang, Y. Chen, D. L. Peng, F. S. Li, and D. S. Xue, *Mater. Lett.* **92**, 346 (2013).
- <sup>16</sup>T. G. Knorr and R. W. Hoffman, *Phys. Rev.* **113**, 1039 (1959).
- <sup>17</sup>N. N. Phuoc, G. Z. Chai, and C. K. Ong, *J. Appl. Phys.* **112**, 083925 (2012).
- <sup>18</sup>X. L. Fan, D. S. Xue, M. Lin, Z. M. Zhang, D. W. Guo, C. J. Jiang, and J. Q. Wei, *Appl. Phys. Lett.* **92**, 222505 (2008).
- <sup>19</sup>Z. M. Zhang, X. L. Fan, M. Lin, D. W. Guo, G. Z. Chai, and D. S. Xue, *J. Phys. D: Appl. Phys.* **43**, 085002 (2010).
- <sup>20</sup>S. D. Li, Z. G. Huang, J. G. Duh, and M. Yamaguchi, *Appl. Phys. Lett.* **92**, 092501 (2008).
- <sup>21</sup>N. N. Phuoc and C. K. Ong, *Adv. Mater.* **25**, 980 (2013).
- <sup>22</sup>N. N. Phuoc and C. K. Ong, *Appl. Phys. Lett.* **102**, 212406 (2013).
- <sup>23</sup>G. Z. Chai, N. N. Phuoc, and C. K. Ong, *Sci. Rep.* **2**, 832 (2012).
- <sup>24</sup>G. Z. Chai, N. N. Phuoc, and C. K. Ong, *Appl. Phys. Lett.* **103**, 042412 (2013).
- <sup>25</sup>G. Z. Chai, N. N. Phuoc, and C. K. Ong, *J. Phys. D: Appl. Phys.* **46**, 415001 (2013).
- <sup>26</sup>G. Z. Chai, N. N. Phuoc, and C. K. Ong, *Appl. Phys. Express* **7**, 063001 (2014).
- <sup>27</sup>T. L. Gilbert, *IEEE Trans. Magn.* **40**, 3443 (2004).
- <sup>28</sup>A. Neudert, J. McCord, R. Schäfer, and L. Schultz, *J. Appl. Phys.* **95**, 6595 (2004).
- <sup>29</sup>V. Bekker, K. Seemann, and H. Leiste, *J. Magn. Magn. Mater.* **270**, 327 (2004).
- <sup>30</sup>Y. Liu, L. F. Chen, C. Y. Tan, H. J. Liu, and C. K. Ong, *Rev. Sci. Instrum.* **76**, 063911 (2005).
- <sup>31</sup>J. L. Snoek, *Physica* **14**, 207 (1948).
- <sup>32</sup>N. N. Phuoc, G. Chai, and C. K. Ong, *J. Appl. Phys.* **112**, 113908 (2012).
- <sup>33</sup>E. Yu, J. S. Shim, I. Kim, J. Kim, S. H. Han, H. J. Kim, K. H. Kim, and M. Yamaguchi, *IEEE Trans. Magn.* **41**, 3259 (2005).